HHS Public Access

Author manuscript

Hum Mutat. Author manuscript; available in PMC 2015 October 16.

Published in final edited form as:

Hum Mutat. 2015 January ; 36(1): 106–117. doi:10.1002/humu.22718.

Variants in *CUL4B* are Associated with Cerebral Malformations

Anneke T. Vulto-van Silfhout[1,†], **Tadashi Nakagawa**[2,†], **Nadia Bahi-Buisson**[3,4,5,†], **Stefan A. Haas**[6], **Hao Hu**[7], **Melanie Bienek**[7], **Lisenka E.L.M. Vissers**[1], **Christian Gilissen**[1], **Andreas Tzschach**[7,8], **Andreas Busche**[9], **Jörg Müsebeck**[10], **Patrick Rump**[11], **Inge B. Mathijssen**[12], **Kristiina Avela**[13], **Mirja Somer**[13], **Fatma Doagu**[14], **Anju K. Philips**[14], **Anita Rauch**[15], **Alessandra Baumer**[15], **Krysta Voesenek**[1], **Karine Poirier**[4,5], **Jacqueline Vigneron**[16], **Daniel Amram**[17], **Sylvie Odent**[18], **Magdalena Nawara**[19], **Ewa Obersztyn**[19], **Jacek Lenart**[19], **Agnieszka Charzewska**[19], **Nicolas Lebrun**[4,5], **Ute Fischer**[7], **Willy M. Nillesen**[1], **Helger G. Yntema**[1], **Irma Järvelä**[14], **Hans-Hilger Ropers**[7], **Bert B.A. de Vries**[1,20], **Han G. Brunner**[1], **Hans van Bokhoven**[1,20], **F. Lucy Raymond**[21], **Michèl A.A.P. Willemsen**[22], **Jamel Chelly**[4,5], **Yue Xiong**[2], **A. James Barkovich**[23], **Vera M. Kalscheuer**[7,*,†], **Tjitske Kleefstra**[1,20,*,†], and **Arjan P.M. de Brouwer**[1,20,†]

[1]Department of Human Genetics, Radboud Institute for Molecular Life Sciences and Donders Institute for Brain, Cognition and Behaviour, Radboud university medical center, Nijmegen, The Netherlands [2]Department of Biochemistry and Biophysics, University of North Carolina at Chapel Hill, Chapel Hill, North Carolina [3]Neurologie pédiatrique, Hopital Necker Enfants Malades, Université Paris Descartes, APHP, Paris, France [4]Institut Cochin, Université Paris-Descartes, CNRS (UMR 8104), Paris, France [5]Inserm, U1016, Paris, France [6]Department of Computational Molecular Biology, Max Planck Institute for Molecular Genetics, Berlin, Germany [7]Department of Human Molecular Genetics, Max Planck Institute for Molecular Genetics, Berlin, Germany [8]Institute of Human Genetics, University of Tuebingen, Tuebingen, Germany [9]Institute of Human Genetics, University Medical Center Freiburg, Freiburg, Germany [10]Centre for Human Genetics, University of Bremen, Bremen, Germany [11]Department of Genetics, University of Groningen, University Medical Center Groningen, Groningen, The Netherlands [12]Department of Clinical Genetics, Academic Medical Center, Amsterdam, The Netherlands [13]Norio Center, Rinnekoti Foundation, Helsinki, Finland [14]Department of Medical Genetics, University of Helsinki, Helsinki, Finland [15]Institute of Medical Genetics, University of Zurich, Schlieren, Switzerland [16]Department of Human Genetics, Regional Maternity University Adolphe Pinard, Nancy, France [17]Department of Human Genetics, Creteil, France [18]Department of Clinical Genetics, CHU Rennes, UMR 6290 CNRS, Université of Rennes, Rennes, France [19]Department of Medical Genetics, Institute of Mother and Child, Warsaw, Poland [20]Department of Cognitive Neurosciences, Donders Institute for Brain, Cognition and Behaviour, Radboud University Nijmegen, Nijmegen, The Netherlands

[*]Correspondence to: Tjitske Kleefstra, Department of Human Genetics 836, Radboud Institute for Molecular Life Sciences and Donders Institute for Brain, Cognition and Behaviour, Radboud university medical center, P.O. Box 9101, 6500 HB Nijmegen, The Netherlands. Tjitske.Kleefstra@radboudumc.nl; Vera M. Kalscheuer, Department of Human Molecular Genetics, Max Planck Institute for Molecular Genetics, Ihnestrasse 73, D-14195 Berlin, Germany. kalscheu@molgen.mpg.de.
[†]These first authors and senior authors contributed equally to this work.

Additional Supporting Information may be found in the online version of this article.

Disclosure statement: The authors declare no conflict of interest. The funders had no role in design, conduct, analysis, and reporting of this study.

[21]Department of Medical Genetics, University of Cambridge, Cambridge, United Kingdom [22]Department of Pediatric Neurology, Radboud university medical center, Nijmegen, The Netherlands [23]Departments of Radiology, Neurology, Pediatrics and Neurosurgery, University of California San Francisco, San Francisco, California

Abstract

Variants in *cullin 4B* (*CUL4B*) are a known cause of syndromic X-linked intellectual disability. Here, we describe an additional 25 patients from 11 families with variants in *CUL4B*. We identified nine different novel variants in these families and confirmed the pathogenicity of all nontruncating variants. Neuroimaging data, available for 15 patients, showed the presence of cerebral malformations in ten patients. The cerebral anomalies comprised malformations of cortical development (MCD), ventriculomegaly, and diminished white matter volume. The phenotypic heterogeneity of the cerebral malformations might result from the involvement of CUL-4B in various cellular pathways essential for normal brain development. Accordingly, we show that CUL-4B interacts with WDR62, a protein in which variants were previously identified in patients with microcephaly and a wide range of MCD. This interaction might contribute to the development of cerebral malformations in patients with variants in *CUL4B*.

Keywords

CUL4B; WDR62; cortical dysplasia; hydrocephalus; intellectual disability; mutation

Introduction

Variants in *cullin 4B* (*CUL4B*; MIM #300304) are a known cause of syndromic X-linked intellectual disability (XLID) [Tarpey et al., 2007; Zou et al., 2007], includingCabezas syndrome (MIM#300354) [Cabezas et al., 2000]. So far, 13 families with 12 unique *CUL4B* variants have been reported [Wei et al., 1993; Cabezas et al., 2000; Vitale et al., 2001; Tarpey et al., 2007; Zou et al., 2007; Badura-Stronka et al., 2010; Isidor et al., 2010; Ravn et al., 2012; Londin et al., 2014]. Tarpey et al. [2007] estimated the frequency of *CUL4B* variants leading to XLID to be around 3% based on a screen of 250 families. The overlapping phenotype in patients with *CUL4B* variants consists of intellectual disability (ID), seizures, tremors, gait abnormalities, behavioral problems, macrocephaly, short stature, obesity, hypogonadotrophic hypogonadism, and variable dysmorphic features.

CUL4B encodes CUL-4B, a member of the cullin protein family [Sarikas et al., 2011]. Cullin proteins form, together with a really interesting new gene (RING)-finger protein, a cullin–RING ligase (CRL) complex that has E3 ubiquitin ligase activity [Jackson and Xiong, 2009]. E3 ubiquitin ligases are involved in the last step of protein ubiquitination, which usually results in degradation of its substrates by the proteasome [Pickart, 2001]. CUL-4B does not interact with its substrate directly, but through a linker protein, DNA damage-binding protein 1 (DDB1), which binds to a substrate-recognition protein [Angers et al., 2006]. Various specific substrate-recognition proteins are known for the CRL4B through which CUL-4B is considered to be involved in the regulation of numerous proteins. Highly

predictive of binding to DDB1 is the presence of a DDB1-binding WD40 (DWD) box [He et al., 2006]. Such a DWD box was previously identified in lissencephaly-1 protein (LIS-1) [Higa et al., 2006], variants in which result in lissencephaly [Lo Nigro et al., 1997]. Furthermore, WD repeat-containing protein 62 (WDR62), variants in which lead to microcephaly and a wide range of malformations of cortical development (MCD) [Bilguvar et al., 2010; Nicholas et al., 2010; Yu et al., 2010; Bhat et al., 2011], is also predicted to have a DWD box. The potential interaction of LIS-1 and/or WDR62 with CUL-4B suggests that CUL-4B might also be involved in regulation of proper brain development. Moreover, Cul-4b was recently implicated in proliferation and organization of neuronal cells [Chen et al., 2012; Liu et al., 2012]. Although macrocephaly is a frequently observed feature in patients with *CUL4B* variants, so far no detailed description of brain abnormalities has been published.

Here, we provide detailed genotype and phenotype information of 25 patients from 11 families with variants in *CUL4B*. We specifically studied the consequences of *CUL4B* variants on brain development. We collected neuroimaging data of a cohort of 15 patients with pathogenic variants in *CUL4B*. In addition, we investigated a possible interaction between CUL-4B and WDR62 or LIS-1.

Patients and Methods

Identification of *CUL4B* Variants in Patients with XLID

Eight families with variants in *CUL4B* (NM_003588.3; NP_003579.3) were identified by massive parallel sequencing in a cohort of 407 families with XLID at the Department of Human Molecular Genetics, Max Planck Institute for Molecular Genetics, Berlin, Germany (Supp. Methods). Detailed clinical data were collected of 20 patients from these eight families and of two patients from one family with a deletion upstream of exon 2 of *CUL4B* (chrX:119,578,701–119,584,448, NCBI36, Hg18) previously described by Whibley et al. [2010]. This study was approved by the institutional review board Commissie Mensgebonden Onderzoek Regio Arnhem-Nijmegen. Written informed consent was obtained for all patients according to the World Medical Association Declaration of Helsinki.

Identification of *CUL4B* Variants in Patients with Cortical Malformations

We studied a cohort of 29 patients with diverse MCD, including one affected brother pair from nonconsanguineous parents. The MCD of these patients consisted of polymicrogyria (PMG) (in 16 patients), the lissencephaly spectrum (in ten patients), or cortical dysplasia (in three patients). In 17 patients, massive parallel sequencing was performed (Supp. Methods). The other 12 patients were examined for *CUL4B* variants by Sanger sequencing.

Review of Neuroimaging Data of Patients with *CUL4B* Variants

All neuroradiological data, available of 12 patients from seven of the XLID families and of the three patients from two families with MCD, were systematically reevaluated by two independent experts (N.B.B. and A.J.B.).

Sanger Sequencing

Validation of variants and sequencing of the coding exons of the *CUL4B* gene was performed using Sanger sequencing on DNA extracted from peripheral blood. Primer sequences and conditions for PCR are available upon request. PCR products were sequenced using the ABI PRISM BigDye Terminator Cycle Sequencing V2.0 Ready Reaction Kit and analyzed with the ABI PRISM 3730 DNA analyzer (Applied Biosystems, Foster City, CA). DNA of all available family members was analyzed for the variant found in the index patient to confirm the segregation of the variant with the disease. Nucleotide numbering uses +1 as the A of the ATG translation initiation codon in the reference sequence (NM_003588.3, NP_003579.3), with the initiation codon as codon 1. All variants identified in this study have been submitted to http://www.lovd.nl/CUL4B.

RT-PCR Analysis

RNA was isolated from Epstein–Barr Virus transformed lymphoblastoid cell lines by using the NucleoSpin RNA II kit (Macherey-Nagel, Düren, Germany) according to manufacturer's protocols. The integrity of the RNA was assessed on 1.2% nondenaturing agarose gel, and the concentration and purity determined by nanodrop 1000 photospectrometer (Thermo Scientific, Waltham, MA). The OD_{260}/OD_{230} and OD_{260}/OD_{280} ratios were in between 1.8 and 2.0. Five hundred nanograms of total RNA was transcribed into cDNA by using the iScript cDNA synthesis kit (Bio-Rad Laboratories, Hercules, CA) according to manufacturer's protocol. Primer sequences and PCR conditions for reverse transcriptase PCR of *CUL4B* are available on request. Reverse transcriptase PCR products were assessed by agarose gel analysis and subsequently sequenced using the ABI PRISM BigDye Terminator Cycle Sequencing V2.0 Ready Reaction Kit and analyzed with the ABI PRISM 3730 DNA analyzer (Applied Biosystems).

Plasmid Construction and Transfection

HEK293T cells stably expressing wild-type (WT) or mutant FLAG-tagged CUL-4B were created as described in the Supp. Methods.

Immunoprecipitation

Cells were washed with phosphate-buffered saline (PBS) and lysed in NP-40 lysis buffer (0.5% Nonidet P-40, 50 mM Tris (pH 7.5), 150 mM NaCl, 10% glycerol and protease inhibitor cocktail) at 4°C for 5 min. Crude lysates were cleared by centrifugation at 17,000 × *g* at 4°C for 15 min, and supernatants were incubated with FLAG M2-agarose (Sigma, St. Louis, MO). The immunocomplexes were washed three times with wash buffer (0.1% Triton X-100, 10% glycerol in PBS) and then subjected to SDS-PAGE.

Cycloheximide Chase Experiment

Cells were treated with cycloheximide (50 μg/ml) for 0 to 6 hr, and then lysed with radioimmunoprecipitation assay buffer (50 mM Tris [pH 8.0], 0.1% SDS, 150 mM NaCl, 1% Nonidet P-40, 0.5% sodium deoxycholate, and protease inhibitor cocktail) at 4°C for 5 min. Crude lysates were cleared by centrifugation at 17,000 × *g* at 4°C for 15 min, and supernatants were subjected to immunoblot analysis.

Immunofluorescence Staining

U2OS cells grown on glass coverslips were transfected using Fugene 6 transfection reagent (Roche, Indianapolis, IN) according to manufacturer's instruction and subsequently prepared for immunostaining. In brief, the cells were fixed for 10 min at −20°C with methanol and then incubated for 1 hr at room temperature with lab-made anti-FLAG antibody containing 1.0% bovine serum albumin and 0.5% Triton X-100, and then for 1 hr at room temperature with rhodamine-labeled goat polyclonal antibody to mouse immunoglobulin (Molecular Probes, Grand Island, NY) at a dilution of 1:2,000. After washing the cells with PBS containing Triton X-100, 5 μg/ml 4′,6-diamidino-2-phenylindole was added for 1 min at room temperature after which cells were examined with fluorescence microscope.

Antibodies

The antibodies used were anti-FLAG M2-HRP antibody (A8592; Sigma), anti-SGN5 (sc-13157; Santa Cruz, Paso Robles, CA), anti-tubulin (MS-581-P0; NeoMarkers, Fremont, CA), anti-WD repeat-containing protein 5 (anti-WDR5) (ab22512, Abcam, Cambridge, England), anti-WDR62 (A301–560A; Bethyl, Montgomery, TX), anti-LIS1 antibody (AB5413, Millipore, Billerica, MA), anti-RBX1, and anti-DDB1 (both generated as described previously [Ohta et al., 1999; Hu et al., 2004]).

Results

Cerebral Abnormalities in Patients with *CUL4B* Variants

Variants in *CUL4B* were detected in eight families (families 1–8) by massive parallel sequencing of 407 families with XLID (2.0% of the entire cohort). Neuroimaging data were available for 11 patients from six of these families and for one patient from a previously reported family with a deletion just upstream of exon 2 (family 9) [Whibley et al., 2010]. Cerebral abnormalities consisting of MCD, ventriculomegaly, and a decrease in white matter volume of variable extent were observed in seven of these 12 patients. We subsequently screened a group of 29 patients (27 sporadic cases and one affected brother pair) with MCD for variants in *CUL4B*. This analysis revealed an additional three patients from two families (families 10–11) with a pathogenic variant in *CUL4B*.

In total, we identified ten patients with *CUL4B* variants and variable cerebral abnormalities (Table 1, Fig. 1). The most severe end of the spectrum consisted of severe ventriculomegaly in combination with bilateral persylvian PMG or a simplified gyral pattern with a slightly thickened cortex (family 1, individual IV:3 and family 10, individuals II:1 and II:2, respectively; Fig. 1A–E). In family 1, ventriculomegaly was also present in the other two patients for whom magnetic resonance imaging (MRI) images were not available. Three of the five patients with severe ventriculomegaly required shunt placement to reduce the increased intracranial pressure due to excess cerebrospinal fluid. The intermediate stage, present in two other unrelated patients, showed a cortical dysplasia of the right hemisphere parietal (family 4, individual III:1) or bilateral perisylvian PMG (family 11, individual II:2; Fig. 1F and G). At the mild end of the spectrum, the cerebral anomalies were more subtle. Individual III:1 of family 2 and the two brothers of family 5 (III:1 and III:2) showed mildly diminished white matter volume and mild ventriculomegaly (Fig. 1H and I). Other brain

abnormalities that were observed consisted of a thin corpus callosum (in three patients), cerebellar vermis atrophy (in two patients), hyperintensity of the white matter (in two patients), persistent cavum septum pellucidum, cavum veli interpositi, geminolytic cysts, and small thalami, hippocampi, pons, and cerebral peduncles.

Clinical Phenotype of Patients with *CUL4B* Variants

Detailed clinical information was available of 22 patients from the nine families from the XLID cohort and of the three patients from the two families from the MCD cohort. The age of the patients ranged from two to 45 years. The clinical phenotype of the patients with the *CUL4B* variants overlapped with that of previously described patients (Table 2 and Supp. clinical reports). ID, which was usually moderate with a disproportionately severely affected speech development, was present in all patients. Other neurological problems were also frequently noted, such as behavioral problems (59%), gait abnormalities (48%), tremors (45%), and seizures (32%). Additional prominent features were genital abnormalities including hypogonadism (85%), short stature (77%), small hands (74%), kyphosis (35%), gynecomastia (33%), and macrocephaly (32%). Frequent facial dysmorphisms consisted of a high forehead (76%), a prominent lower lip (78%), and malformed and/or abnormally positioned ears (89%) (Fig. 2). The facial phenotype changed with age. At a younger age, there was often a depressed nasal bridge with a bulbous tip (55%), while at an older age the facial appearance became more coarse, with hyperplastic supraorbital ridges (77%) and prognathia (68%). On the basis of our and previously published clinical data, we developed a guideline that can be used to identify potential patients with *CUL4B* variants (Supp. Table S1).

CUL4B Variants

The *CUL4B* variants identified in this study were spread throughout the gene and consisted of a missense change, an in-frame deletion of three base pairs, an in-frame duplication of three base pairs, two splice site variants, and five truncating variants, including a five base pair deletion (family 4, p.(Ile336Lysfs*2)) that was reported previously in an unrelated family [Tarpey et al., 2007] (Fig. 3). All variants were confirmed by Sanger sequencing and segregated with the disease in the families, except in family 5, in which one intellectually disabled half-brother, who was born from the same mother, did not carry the c.2493+3A>G variant in *CUL4B* (Fig. 3B).

All novel variants were assessed for their pathogenicity. Truncating variants were considered to be pathogenic as described before [Tarpey et al., 2007]. Two variants, c.2493+3A>G (family 5) and c.1906+1G>T (family 7), were predicted to influence normal splicing by MaxEntScan [Yeo and Burge, 2004] and NNSPLICE version 0.9 [Reese et al., 1997]. For c.2493+3A>G, the MAXENT score was reduced from 5.46 to 0.06 and the NNSPLICE donor site prediction score from 0.57 to zero. For c.1906+1G>T, the MAXENT score was reduced from 8.60 to 0.10 and the NNSPLICE donor site prediction score from 0.92 to zero. Both variants were investigated by RT-PCR analysis on cDNA from the index patient. The variant c.2493+3A>G abolished the splice donor site of exon 20, leading to the activation of two cryptic splice donor sites within exon 20, which both resulted in a frameshift and a premature termination codon in exon 21 (Fig. 3C). The variant c.

1906+1G>T abolished the splice donor site of exon 15, which resulted in skipping of exon 15 leading to a deletion of 37 amino acid residues (p.(Gly599 His635del)) within the cullin domain (Fig. 3D).

To determine the effect of the single amino acid changes p.(Leu785del) (family 2), p.(Ala621dup) (family 3), and p.(Pro50Leu) (family 10) on the function of CUL-4B, we analyzed the degradation of WDR5, one of the targets of the CRL4B [Nakagawa and Xiong, 2011], in HEK293T cells stably expressing WT and mutant FLAG-tagged CUL-4B. For all three mutants, the WDR5 protein levels were elevated compared to WT (Fig. 4A). There were no indications that the binding of the mutated CUL-4B to the RING-finger RBX1, DDB1, and COP9 signalosome complex subunit 5 (SGN5), three known interactors of CUL-4B [Sarikas et al., 2011], was significantly affected (Supp. Fig. S1A). Two out of three mutant CUL-4B proteins showed decreased protein stability (Fig. 4B), which might explain the impaired CUL-4B function of these mutants. The missense change p.(Pro50Leu) did not show decreased protein stability, but since this variant is close to the nuclear localization signal (NLS) of *CUL4B*, we hypothesized that this variant may have an impact on the subcellular localization of CUL-4B. However, subcellular localization of all three mutants by immunostaining showed a normal nuclear localization of CUL-4B (Supp. Fig. S1B), suggesting that this mutant impacts CUL-4B function by a different mechanism than affecting protein stability or nuclear localization.

Interaction of CUL-4B with LIS-1 and WDR62

Two proteins that are known to cause cerebral malformations, WDR62 [Bilguvar et al., 2010; Nicholas et al., 2010; Yu et al., 2010] and LIS-1 [Lo Nigro et al., 1997], contain a DWD box sequence (Supp. Fig. S2A), which is predictive of binding to DDB1 [He et al., 2006], an essential component of the CRL4B. Immunoprecipitation (IP) of CUL-4A and CUL-4B in HEK293T cells followed by immunoblot of precipitates showed that WDR62 interacts with CUL-4B, but not with CUL-4A (Fig. 4C). Similar IP experiments investigating a possible interaction of LIS-1 with CUL-4B showed no LIS-1 in the precipitates, suggesting that LIS-1 does not interact with CUL-4B (Supp. Fig. S2B).

It was previously shown for WDR5 that DWD proteins cannot only function as substrate-recognition proteins, but can also be substrates for degradation by CUL-4B themselves [Nakagawa and Xiong, 2011]. Therefore, we investigated whether knockdown of CUL-4B by short-hairpin RNA influenced protein expression of WDR62 and LIS-1. Protein levels of WDR62 and LIS-1 were not influenced by knockdown of CUL-4B, whereas WDR5 levels were influenced by knockdown of CUL-4B, suggesting that WDR62 and LIS-1 are no direct substrates of CUL-4B themselves (Supp. Fig. S2C). Normal protein levels of WDR62 and LIS-1 were also seen for the different mutant FLAG-tagged CUL-4B expressing cells (Fig. 4A).

Discussion

In this article, we describe detailed neuroradiological data of 15 male patients and overall clinical data of 25 patients derived from 11 families with pathogenic variants affecting *CUL4B*. Our data show for the first time a firm association between *CUL4B* variants and

cerebral malformations. Detailed assessment of neuroimaging data showed that cerebral malformations comprising MCD, ventriculomegaly, and diminished white matter volume were present in ten of 15 patients investigated. The *CUL4B*-associated cerebral malformations were of variable severity, the severest form consisting of massive ventriculomegaly in combination with MCD. Known genetic causes of X-linked hydrocephalus (*L1CAM* and *AP1S2*) were excluded in these families. In the remaining patients, the severity of the cerebral malformations ranged from bilateral MCD to more subtle diminished white matter volume and ventricular enlargement. We did not observe a correlation between the type or position of the variant and the severity of the cerebral abnormalities. However, within the three families for whom neuroimaging data were available of multiple affected individuals (families 1, 5, and 10), the cerebral abnormalities were strikingly similar among the different family members, which suggests that there might be a variant-specific effect of the respective *CUL4B* variants on cerebral development.

Cerebral malformations have not been reported to date as a feature associated with *CUL4B* variants, except for one individual from family 43 who was reported to have a porencephalic cyst in the original description of this condition [Tarpey et al., 2007]. However, detailed and systematic neuroimaging analysis of patients with *CUL4B* variants has not been performed until now. Accordingly, MRI analysis of additional affected family members of family 43 has now also shown the presence of abnormalities of the lateral ventricles, corpus callosum, and heterotopic gray matter (F.L. Raymond, personal communication), further supporting our finding that cerebral malformations are a significant feature in patients with *CUL4B* variants.

Our data suggest that CUL-4B plays an important role in brain development. This is supported by the observation of abnormal neuronal organization in the hippocampus in Cul-4b knockout mice [Chen et al., 2012]. Furthermore, Cul-4b was shown to be essential for proliferation of neural progenitor cells in rodents as knockdown of Cul-4b accumulated these cells in the G2/M phase of the cell cycle [Liu et al., 2012]. A general involvement of the cullin family in brain development is further supported by mice with a knockdown of cullin 5, which also show aberrant neuronal migration [Feng et al., 2007].

The identification of an in vivo interaction between CUL-4B and WDR62 provides a possible mechanism for the development of cerebral malformations in patients with a *CUL4B* variant. Homozygous variants in WDR62 result in microcephaly and a wide range of MCD [Bilguvar et al., 2010; Nicholas et al., 2010; Yu et al., 2010; Bhat et al., 2011], including cortical thickening, pachygyria, simplified gyral pattern, PMG, heterotopias, and schizencephaly [Bilguvar et al., 2010; Nicholas et al., 2010; Yu et al., 2010; Bhat et al., 2011]. MCD are also present in five of our patients. However, while variants in *WDR62* lead to severe and profound microcephaly, patients with *CUL4B* variants usually have macrocephaly with ventriculomegaly and diminished white matter volume, although microcephaly has been reported in two families [Wei et al., 1993; Vitale et al., 2001; Zou et al., 2007; Londin et al., 2014]. The interaction with WDR62 is specific for CUL-4B, as IPs with an anti-CUL-4A antibody did not result in coprecipitation of WDR62. The main difference between these paralogues is that CUL-4B has an extended N-terminus, which contains a nuclear localization signal [Zou et al., 2009; Nakagawa and Xiong, 2011]. The

subcellular localization of WDR62 has been reported to be cell cycle and tissue dependent [Bilguvar et al., 2010; Nicholas et al., 2010; Yu et al., 2010; Bhat et al., 2011]. In neuronal cells, WDR62 has been shown to localize predominantly to the nucleus [Bilguvar et al., 2010; Nicholas et al., 2010], suggesting that WDR62 and CUL-4B interact in the nucleus and form a complex necessary for proper cerebral development. We were not able to detect an interaction between LIS-1 and CUL-4B. However, LIS-1 has previously been shown to interact with DDB1 [Higa et al., 2006]. As LIS-1 mainly localizes to the centrosome and the perinuclear region, but not to the nucleus [Tanaka et al., 2004], it could well be that LIS-1 binds to DDB1 in the cytoplasm, but that it does not interact with nuclear CUL-4B. However, we cannot exclude that during cell division CUL-4B is able to interact with LIS-1.

The development of cerebral malformations in patients with *CUL4B* variants might also result from the disturbance of other pathways, as currently more than 20 proteins are known to be substrates of CRL4 ubiquitin ligase complex [Kerzendorfer et al., 2011; Li et al., 2011]. CUL-4B is hypothesized to regulate the mTORC1 signaling pathway, as knockdown of CUL-4B results in decreased phosphorylation of ribosomal protein S6 kinase beta-1 and eukaryotic translation initiation factor 4E-binding protein 1 [Ghosh et al., 2008; Kerzendorfer et al., 2011]. This downregulation is likely mediated by increased stability of DNA damage inducible transcript 4 protein and tuberin, two targets of the CRL4 ubiquitin ligase complex [Hu et al., 2008; Katiyar et al., 2009; Wang et al., 2013]. The mTOR pathway was recently linked to megalencephaly–PMG–polydactyly–hydrocephalus (MPPH) syndrome, which also has the combination of the phenotypic features of MCD and ventriculomegaly. Activating de novo variants in *AKT3*, *PIK3R2*, and *PIK3CA*, three core components of this pathway, were identified in patients with this phenotype [Riviere et al., 2012]. However, knockdown of CUL-4B is currently only associated with downregulation of mTOR signaling, whereas the variants seen in MPPH syndrome were shown to lead to upregulation of this signaling pathway.

Variants in *CUL4B* might also affect chromatin remodeling. Knockdown of CUL-4B results in increased WDR5 levels, a core member of the SET1/MLL family of histone methyltransferase complexes [Dou et al., 2006; Trievel and Shilatifard, 2009]. An increase in WDR5 was previously shown to lead to increased expression of several neuronal genes through increased H3K4me3 levels at their promoters [Nakagawa and Xiong, 2011]. Moreover, CUL-4B can also influence chromatin remodeling through monoubiquitination of histone H2A lysine 119 [Hu et al., 2012; Yang et al., 2013]. Impaired chromatin remodeling, more specifically also increased H3K4 methylation, is a common mechanism underlying ID [van Bokhoven, 2011], for example, in patients with *KDM5C* variants [Iwase et al., 2007; Tahiliani et al., 2007], and is also implicated in cerebral development [Yang et al., 2012].

In conclusion, we show that *CUL4B* variants are associated with a wide range of cerebral malformations such as MCD, ventriculomegaly, and diminished white matter volume. The phenotypic heterogeneity might result from the involvement of CUL-4B in various cellular pathways essential for normal brain development. Accordingly, we show that CUL-4B interacts with WDR62, a protein in which variants were previously identified in patients with microcephaly and a wide range of MCD, providing a potential mechanism for the development of these brain abnormalities in patients with *CUL4B* variants.

Supplementary Material

Refer to Web version on PubMed Central for supplementary material.

Acknowledgments

We are grateful to the patients and their families for their participation. We would like to thank the Department of Radiology, University Medical Center Freiburg for the MRI studies, Carlijn Brekelmans for the overview of cortical malformation genes, Karoline Gemeinhardt and Melanie Hambrock for RT-PCR analysis, and Susanne Freier for excellent technical assistance. A.T.Vv.S, T.N., N.B-.B., Y.X., J.C., V.M.K., T.K., and A.P.Md.B. conceived the project. A.T.Vv.S., S.A.H., H.H., M.B., L.E.V., C.G., A.K.P., K.V., K.P., W.M.N., H.G.Y., U.F., H.H.R., H.v.B., V.M.K., and A.P.M.d.B. were involved in the (X-)exome sequencing, data analysis, and interpretation. A.T.Vv.S., N.B.B., A.T., A.B., J.M., P.R., I.B.M., K.A., M.S., F.D., A.R., A.B., J.V., D.A., S.O., M.N., E.O., J.L., A.C., I.J., B.B.A.d.V., H.G.B., F.L.R., and T.K. were involved in collection of patients with *CUL4B* variants. T.N. and Y.X. performed the experiments on the single amino acid changes and the WDR62 and LIS-1 interactions. N.B.B., M.A.A.P.W., N.L., J.C., and A.J.B. assessed the neuroimaging data. A.T.Vv.S. and A.P.Md.B. prepared the first draft of the manuscript. All authors contributed to the final manuscript.

Contract grant sponsor(s): European Commission (GENCODYS grant 241995 under FP7); Dutch Organisation for Health Research and Development (ZON-MW grant 917-86-319; ZON-MW grant 907-00-365); Dutch Brain Foundation (2009(2)-81); Van Leersum Fund; German Ministry of Education and Research through the MRNET; Max Planck Innovation Funds; Sigrid Juselius Foundation, Helsinki, Finland; NIH grant (GM067113); Action Medical Research and NIHR Biomedical Research Centre, UK; Polish Ministry of Science and Higher Education (NN407133739).

References

Angers S, Li T, Yi X, MacCoss MJ, Moon RT, Zheng N. Molecular architecture and assembly of the DDB1-CUL4A ubiquitin ligase machinery. Nature. 2006; 443:590–593. [PubMed: 16964240]

Badura-Stronka M, Jamsheer A, Materna-Kiryluk A, Sowinska A, Kiryluk K, Budny B, Latos-Bielenska A. A novel nonsense mutation in CUL4B gene in three brothers with X-linked mental retardation syndrome. Clin Genet. 2010; 77:141–144. [PubMed: 20002452]

Bhat V, Girimaji SC, Mohan G, Arvinda HR, Singhmar P, Duvvari MR, Kumar A. Mutations in WDR62, encoding a centrosomal and nuclear protein, in Indian primary microcephaly families with cortical malformations. Clin Genet. 2011; 80:532–540. [PubMed: 21496009]

Bilguvar K, Ozturk AK, Louvi A, Kwan KY, Choi M, Tatli B, Yalnizoglu D, Tuysuz B, Caglayan AO, Gokben S, Kaymakcalan H, Barak T, et al. Whole-exome sequencing identifies recessive WDR62 mutations in severe brain malformations. Nature. 2010; 467:207–210. [PubMed: 20729831]

Cabezas DA, Slaugh R, Abidi F, Arena JF, Stevenson RE, Schwartz CE, Lubs HA. A new X linked mental retardation (XLMR) syndrome with short stature, small testes, muscle wasting, and tremor localises to Xq24-q25. J Med Genet. 2000; 37:663–668. [PubMed: 10978355]

Chen CY, Tsai MS, Lin CY, Yu IS, Chen YT, Lin SR, Juan LW, Chen YT, Hsu HM, Lee LJ, Lin SW. Rescue of the genetically engineered Cul4b mutant mouse as a potential model for human X-linked mental retardation. Hum Mol Genet. 2012; 21:4270–4285. [PubMed: 22763239]

Dou Y, Milne TA, Ruthenburg AJ, Lee S, Lee JW, Verdine GL, Allis CD, Roeder RG. Regulation of MLL1 H3K4 methyltransferase activity by its core components. Nat Struct Mol Biol. 2006; 13:713–719. [PubMed: 16878130]

Feng L, Allen NS, Simo S, Cooper JA. Cullin 5 regulates Dab1 protein levels and neuron positioning during cortical development. Genes Dev. 2007; 21:2717–2730. [PubMed: 17974915]

Ghosh P, Wu M, Zhang H, Sun H. mTORC1 signaling requires proteasomal function and the involvement of CUL4-DDB1 ubiquitin E3 ligase. Cell Cycle. 2008; 7:373–381. [PubMed: 18235224]

He YJ, McCall CM, Hu J, Zeng Y, Xiong Y. DDB1 functions as a linker to recruit receptor WD40 proteins to CUL4-ROC1 ubiquitin ligases. Genes Dev. 2006; 20:2949–2954. [PubMed: 17079684]

Higa LA, Wu M, Ye T, Kobayashi R, Sun H, Zhang H. CUL4-DDB1 ubiquitin ligase interacts with multiple WD40-repeat proteins and regulates histone methylation. Nat Cell Biol. 2006; 8:1277–1283. [PubMed: 17041588]

Hu H, Yang Y, Ji Q, Zhao W, Jiang B, Liu R, Yuan J, Liu Q, Li X, Zou Y, Shao C, Shang Y, et al. CRL4B catalyzes H2AK119 monoubiquitination and coordinates with PRC2 to promote tumorigenesis. Cancer Cell. 2012; 22:781–795. [PubMed: 23238014]

Hu J, McCall CM, Ohta T, Xiong Y. Targeted ubiquitination of CDT1 by the DDB1-CUL4A-ROC1 ligase in response to DNA damage. Nat Cell Biol. 2004; 6:1003–1009. [PubMed: 15448697]

Hu J, Zacharek S, He YJ, Lee H, Shumway S, Duronio RJ, Xiong Y. WD40 protein FBW5 promotes ubiquitination of tumor suppressor TSC2 by DDB1-CUL4-ROC1 ligase. Genes Dev. 2008; 22:866–871. [PubMed: 18381890]

Isidor B, Pichon O, Baron S, David A, Le Caignec C. Deletion of the CUL4B gene in a boy with mental retardation, minor facial anomalies, short stature, hypogonadism, and ataxia. Am J Med Genet A. 2010; 152A:175–180. [PubMed: 20014135]

Iwase S, Lan F, Bayliss P, de la Torre-Ubieta L, Huarte M, Qi HH, Whetstine JR, Bonni A, Roberts TM, Shi Y. The X-linked mental retardation gene SMCX/JARID1C defines a family of histone H3 lysine 4 demethylases. Cell. 2007; 128:1077–1088. [PubMed: 17320160]

Jackson S, Xiong Y. CRL4s: the CUL4-RING E3 ubiquitin ligases. Trends Biochem Sci. 2009; 34:562–570. [PubMed: 19818632]

Katiyar S, Liu E, Knutzen CA, Lang ES, Lombardo CR, Sankar S, Toth JI, Petroski MD, Ronai Z, Chiang GG. REDD1, an inhibitor of mTOR signalling, is regulated by the CUL4A-DDB1 ubiquitin ligase. EMBO Rep. 2009; 10:866–872. [PubMed: 19557001]

Kerzendorfer C, Hart L, Colnaghi R, Carpenter G, Alcantara D, Outwin E, Carr AM, O'Driscoll M. CUL4B-deficiency in humans: understanding the clinical consequences of impaired cullin 4-RING E3 ubiquitin ligase function. Mech Ageing Dev. 2011; 132:366–373. [PubMed: 21352845]

Li X, Lu D, He F, Zhou H, Liu Q, Wang Y, Shao C, Gong Y. Cullin 4B protein ubiquitin ligase targets peroxiredoxin III for degradation. J Biol Chem. 2011; 286:32344–32354. [PubMed: 21795677]

Liu HC, Enikolopov G, Chen Y. Cul4B regulates neural progenitor cell growth. BMC Neurosci. 2012; 13:112. [PubMed: 22992378]

Lo Nigro C, Chong CS, Smith AC, Dobyns WB, Carrozzo R, Ledbetter DH. Point mutations and an intragenic deletion in LIS1, the lissencephaly causative gene in isolated lissencephaly sequence and Miller-Dieker syndrome. Hum Mol Genet. 1997; 6:157–164. [PubMed: 9063735]

Londin ER, Adijanto J, Philp N, Novelli A, Vitale E, Perria C, Serra G, Alesi V, Surrey S, Fortina P. Donor splice-site mutation in CUL4B is likely cause of X-linked intellectual disability. Am J Med Genet A. 2014; 164A:2294–2299. [PubMed: 24898194]

Nakagawa T, Xiong Y. X-linked mental retardation gene CUL4B targets ubiquitylation of H3K4 methyltransferase component WDR5 and regulates neuronal gene expression. Mol Cell. 2011; 43:381–391. [PubMed: 21816345]

Nicholas AK, Khurshid M, Desir J, Carvalho OP, Cox JJ, Thornton G, Kausar R, Ansar M, Ahmad W, Verloes A, Passemard S, Misson JP, et al. WDR62 is associated with the spindle pole and is mutated in human microcephaly. Nat Genet. 2010; 42:1010–1014. [PubMed: 20890279]

Ohta T, Michel JJ, Schottelius AJ, Xiong Y. ROC1, a homolog of APC11, represents a family of cullin partners with an associated ubiquitin ligase activity. Mol Cell. 1999; 3:535–541. [PubMed: 10230407]

Pickart CM. Mechanisms underlying ubiquitination. Annu Rev Biochem. 2001; 70:503–533. [PubMed: 11395416]

Ravn K, Lindquist S, Nielsen K, Dahm T, Tumer Z. Deletion of CUL4B leads to concordant phenotype in a monozygotic twin pair. Clin Genet. 2012; 82:292–294. [PubMed: 22182342]

Reese MG, Eeckman FH, Kulp D, Haussler D. Improved splice site detection in Genie. J Comput Biol. 1997; 4:311–323. [PubMed: 9278062]

Riviere JB, Mirzaa GM, O'Roak BJ, Beddaoui M, Alcantara D, Conway RL, St-Onge J, Schwartzentruber JA, Gripp KW, Nikkel SM, Worthylake T, Sullivan CT, et al. De novo germline and postzygotic mutations in AKT3, PIK3R2 and PIK3CA cause a spectrum of related megalencephaly syndromes. Nat Genet. 2012; 44:934–940. [PubMed: 22729224]

Sarikas A, Hartmann T, Pan ZQ. The cullin protein family. Genome Biol. 2011; 12:220. [PubMed: 21554755]

Tahiliani M, Mei P, Fang R, Leonor T, Rutenberg M, Shimizu F, Li J, Rao A, Shi Y. The histone H3K4 demethylase SMCX links REST target genes to X-linked mental retardation. Nature. 2007; 447:601–605. [PubMed: 17468742]

Tanaka T, Serneo FF, Higgins C, Gambello MJ, Wynshaw-Boris A, Gleeson JG. Lis1 and doublecortin function with dynein to mediate coupling of the nucleus to the centrosome in neuronal migration. J Cell Biol. 2004; 165:709–721. [PubMed: 15173193]

Tarpey PS, Raymond FL, O'Meara S, Edkins S, Teague J, Butler A, Dicks E, Stevens C, Tofts C, Avis T, Barthorpe S, Buck G, et al. Mutations in CUL4B, which encodes a ubiquitin E3 ligase subunit, cause an X-linked mental retardation syndrome associated with aggressive outbursts, seizures, relative macrocephaly, central obesity, hypogonadism, pes cavus, and tremor. Am J Hum Genet. 2007; 80:345–352. [PubMed: 17236139]

Trievel RC, Shilatifard A. WDR5, a complexed protein. Nat Struct Mol Biol. 2009; 16:678–680. [PubMed: 19578375]

van Bokhoven H. Genetic and epigenetic networks in intellectual disabilities. Annu Rev Genet. 2011; 45:81–104. [PubMed: 21910631]

Vitale E, Specchia C, Devoto M, Angius A, Rong S, Rocchi M, Schwalb M, Demelas L, Paglietti D, Manca S, Mastropaolo C, Serra G. Novel X-linked mental retardation syndrome with short stature maps to Xq24. Am J Med Genet. 2001; 103:1–8. [PubMed: 11562927]

Wang HL, Chang NC, Weng YH, Yeh TH. XLID CUL4B mutants are defective in promoting TSC2 degradation and positively regulating mTOR signaling in neocortical neurons. Biochim Biophys Acta. 2013; 1832:585–593. [PubMed: 23348097]

Wei J, Chen B, Jiang Y, Yang Y, Guo Y. Smith-Fineman-Myers syndrome: report on a large family. Am J Med Genet. 1993; 47:307–311. [PubMed: 8135271]

Whibley AC, Plagnol V, Tarpey PS, Abidi F, Fullston T, Choma MK, Boucher CA, Shepherd L, Willatt L, Parkin G, Smith R, Futreal PA, et al. Fine-scale survey of X chromosome copy number variants and indels underlying intellectual disability. Am J Hum Genet. 2010; 87:173–188. [PubMed: 20655035]

Yang Y, Liu R, Qiu R, Zheng Y, Huang W, Hu H, Ji Q, He H, Shang Y, Gong Y, Wang Y. CRL4B promotes tumorigenesis by coordinating with SUV39H1/HP1/DNMT3A in DNA methylation-based epigenetic silencing. Oncogene. 2013

Yang YJ, Baltus AE, Mathew RS, Murphy EA, Evrony GD, Gonzalez DM, Wang EP, Marshall-Walker CA, Barry BJ, Murn J, Tatarakis A, Mahajan MA, et al. Microcephaly gene links trithorax and REST/NRSF to control neural stem cell proliferation and differentiation. Cell. 2012; 151:1097–1112. [PubMed: 23178126]

Yeo G, Burge CB. Maximum entropy modeling of short sequence motifs with applications to RNA splicing signals. J Comput Biol. 2004; 11:377–394. [PubMed: 15285897]

Yu TW, Mochida GH, Tischfield DJ, Sgaier SK, Flores-Sarnat L, Sergi CM, Topcu M, McDonald MT, Barry BJ, Felie JM, Sunu C, Dobyns WB, et al. Mutations in WDR62, encoding a centrosome-associated protein, cause microcephaly with simplified gyri and abnormal cortical architecture. Nat Genet. 2010; 42:1015–1020. [PubMed: 20890278]

Zou Y, Liu Q, Chen B, Zhang X, Guo C, Zhou H, Li J, Gao G, Guo Y, Yan C, Wei J, Shao C, et al. Mutation in CUL4B, which encodes a member of cullin-RING ubiquitin ligase complex, causes X-linked mental retardation. Am J Hum Genet. 2007; 80:561–566. [PubMed: 17273978]

Zou Y, Mi J, Cui J, Lu D, Zhang X, Guo C, Gao G, Liu Q, Chen B, Shao C, Gong Y. Characterization of nuclear localization signal in the N terminus of CUL4B and its essential role in cyclin E degradation and cell cycle progression. J Biol Chem. 2009; 284:33320–33332. [PubMed: 19801544]

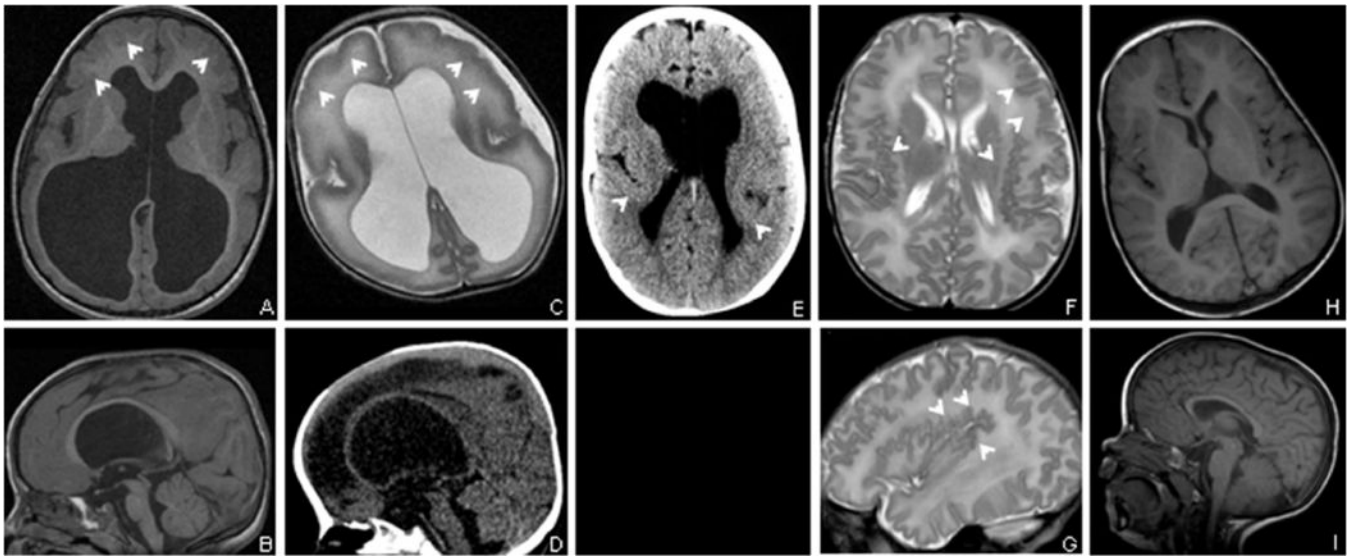

Figure 1.

Representative MRI and computed tomography (CT) images from patients with *CUL4B* variants. **A** and **B**: Family 10—individual II-1 (2.5 years): MRI T1 axial (**A**) and sagittal (**B**) sections show severe ventricular enlargement (colpocephaly), arched and thin corpus callosum, and a slightly thick and undersulcated cortex (arrows). **C** and **D**: Family 10—individual II-2 (6 months, before placement of VP-shunt): MRI T2 axial (**C**) and CT scan sagittal (**D**) sections show severe ventricular enlargement, arched and thin corpus callosum, and a very simplified gyral pattern (arrows). **E**: Family 1—individual IV-3 (6 weeks): CT scan axial section shows severe ventricular enlargement and bilateral perisylvian PMG (arrows). **F** and **G**: Family 11—individual II-2 (Day 13): T2 axial section (**F**) and parasagittal section through left perisylvian area (**G**) show bilateral perisylvian PMG (arrows). **H** and **I**: Family 2—individual III-1 (2 years): T1 axial (**H**), and sagittal (**I**) sections show a mild predominantly posterior ventriculomegaly and a thin corpus callosum.

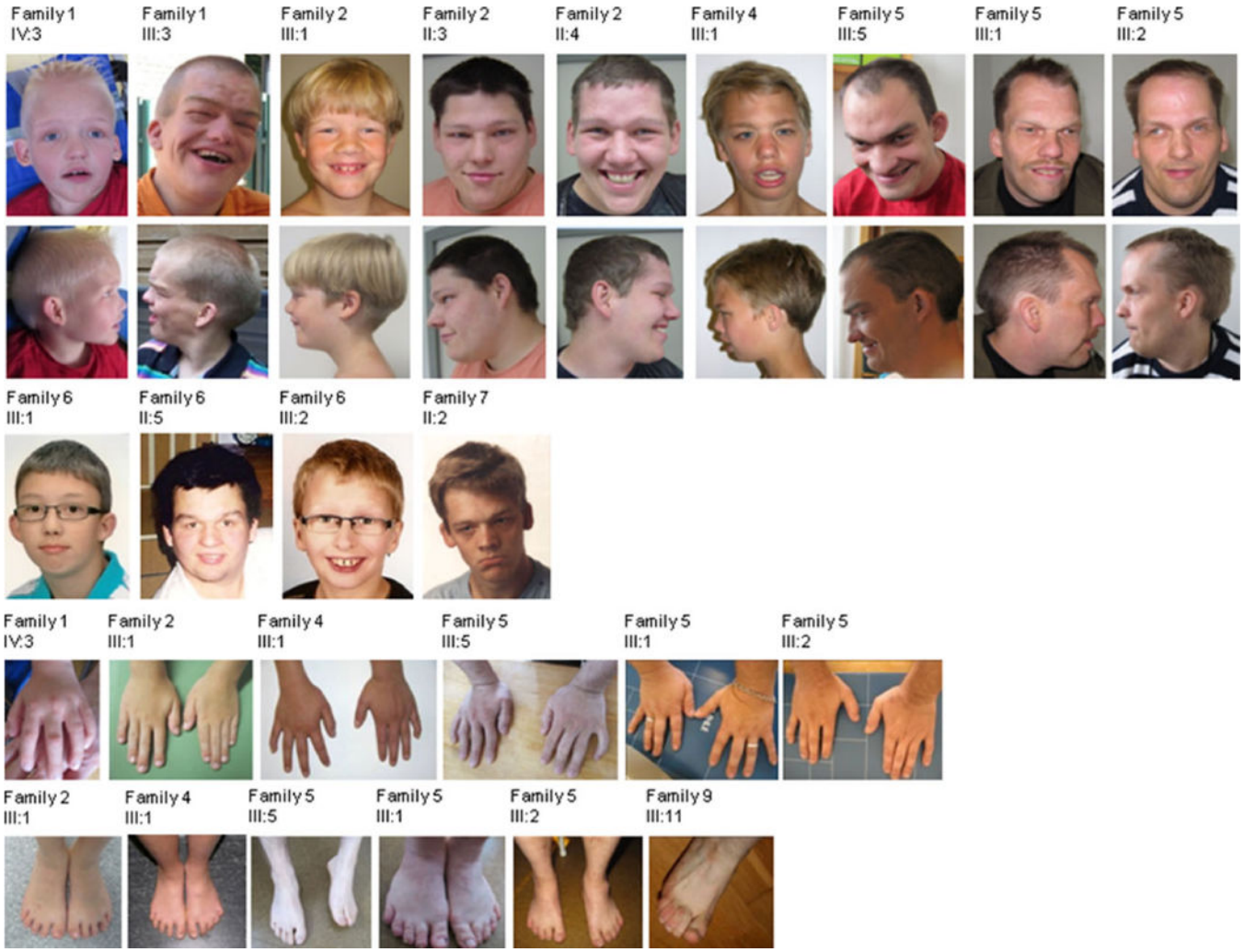

Figure 2.

Images of patients with *CUL4B* variants. Recurrent facial dysmorphisms include high/prominent forehead, malformed, and abnormally positioned ears, hyperplastic supraorbital ridges/deep-set eyes with narrow palpebral fissures, low nasal bridge with a rounded nasal tip, prominent lower lip, and prognathia. Extremities show small hands/feet with brachydactyly, clinodactyly, syndactyly 2–3 of toes, and sandal gap. For description of dysmorphisms, see Table 2.

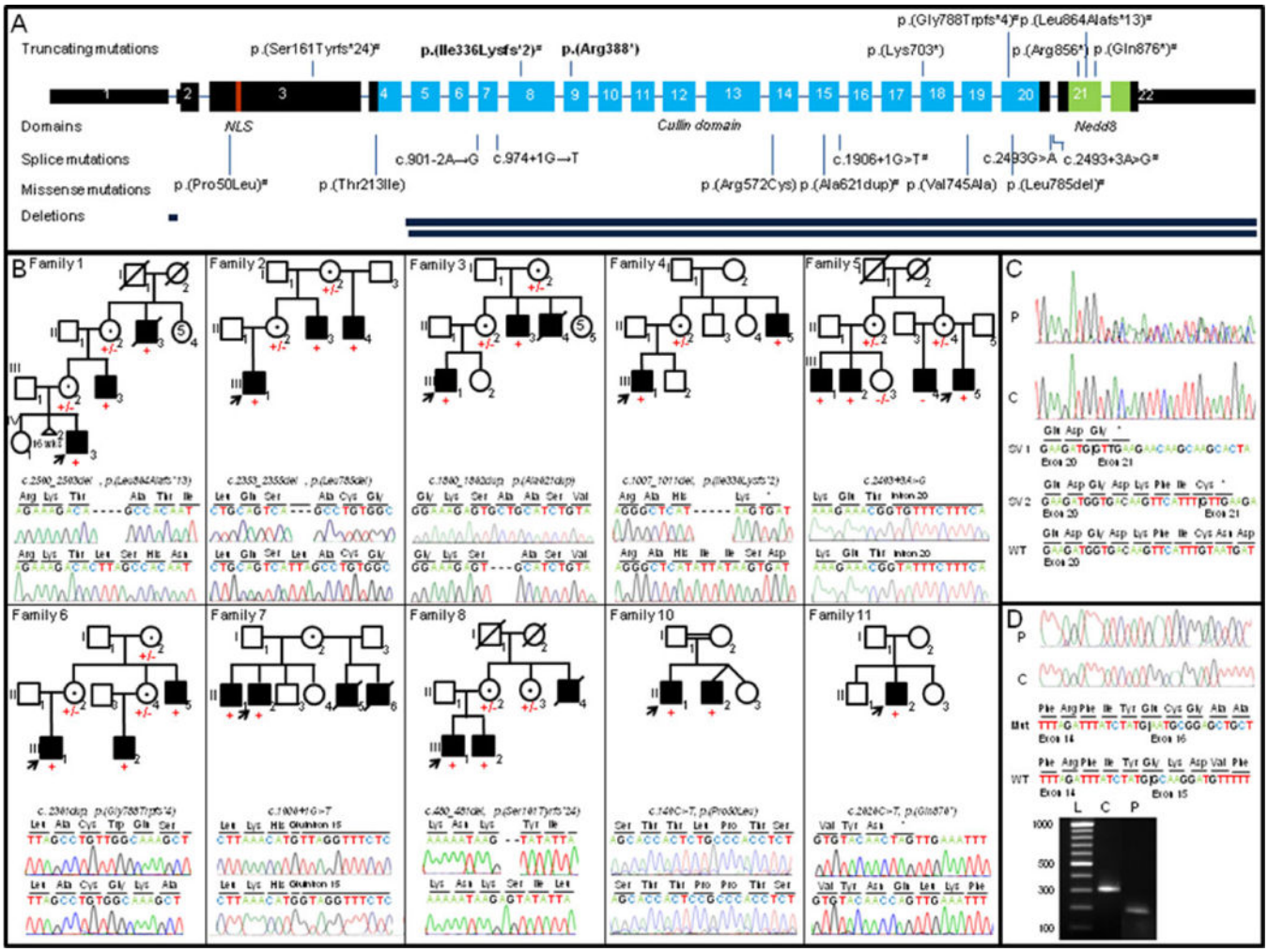

Figure 3.

Overview of *CUL4B* variants identified in this study. **A**: Schematic overview of the *CUL4B* gene including the 22 exons and known domains. The positions of all previously described variants [Tarpey et al., 2007; Zou et al., 2007; Badura-Stronka et al., 2010; Isidor et al., 2010; Whibley et al., 2010; Ravn et al., 2012; Londin et al., 2014] and novel variants are depicted. Recurrent variants are depicted in bold; novel variants from this study are marked with a hash (#). Nuclear localization signal (NLS) is shown in red, cullin domain in blue, and neddylation domain (Nedd8) in green. **B**: Pedigrees of families with *CUL4B* variant and results from segregation studies. Mutant alleles are represented by a plus (+) and WT alleles by a minus (−). Arrows indicate probands. Below each pedigree, Sanger sequencing chromatograms of the proband (top) and a control (bottom) are depicted. **C**: RT-PCR analysis of *CUL4B* splice site variant of family 5. Alternative splicing occurs between exon 20 and 21. Two alternative splice donor sites within exon 20 are used, which result in premature termination codons at amino acid position 806 (splice variant 1; SV1) and 811 (SV2), respectively. P, patient; C, control. **D**: RT-PCR analysis of *CUL4B* splice site variant of family 7. The variant leads to skipping of exon 15, which results in a 111 base pair

shorter transcript as confirmed by agarose gel electrophoresis and subsequent Sanger sequencing. L, DNA size ladder; P, patient; C, control.

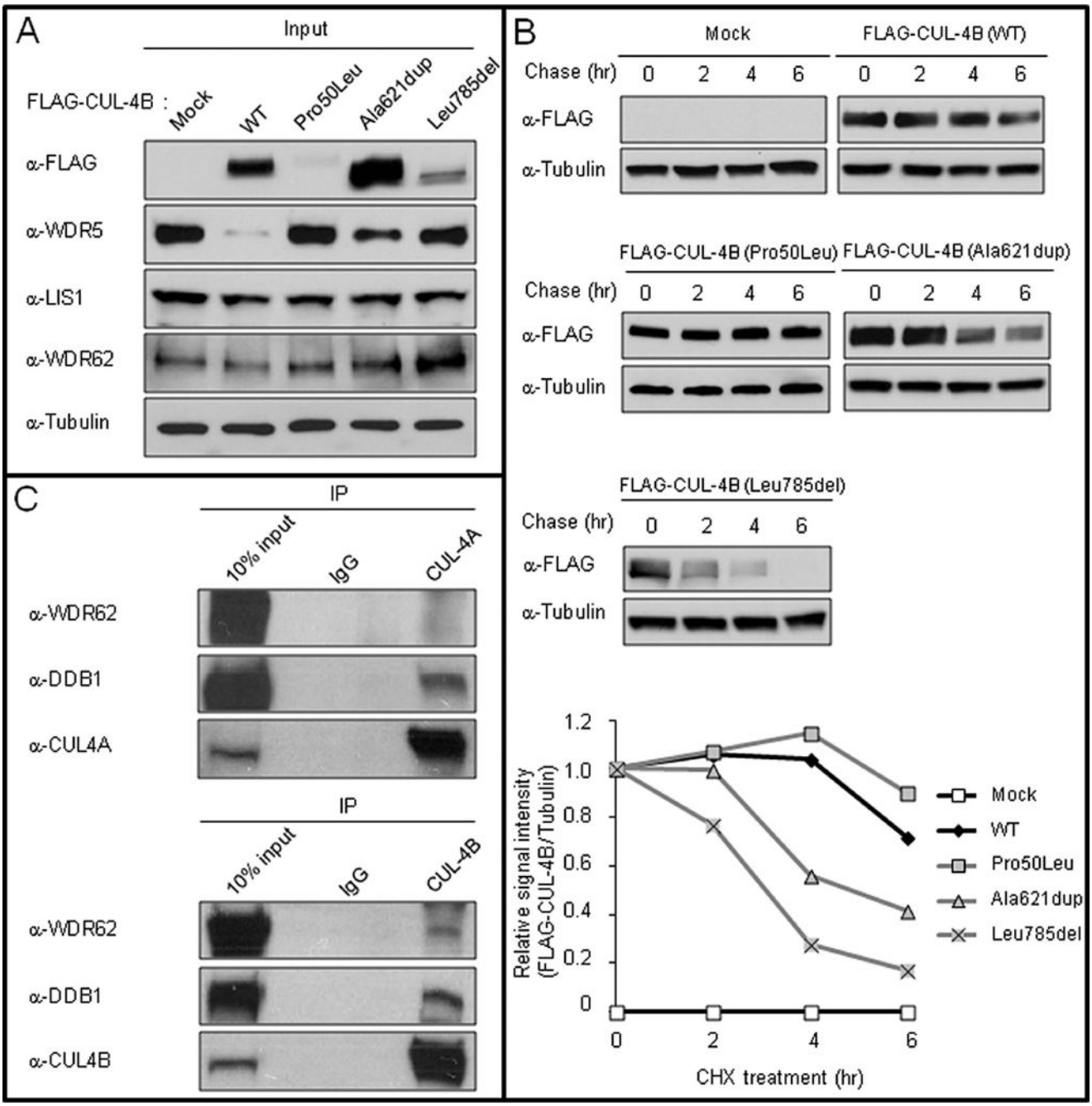

Figure 4.

Effect of the novel amino acid altering variants p.(Leu785del), p.(Ala621dup), and p.(Pro50Leu) on the function of CUL-4B (**A** and **B**) and interaction of normal CUL-4B with WDR62 (**C**). **A**: Western blot showing the WDR5, LIS-1, and WDR62 protein levels in HEK293T cells expressing WT, p.(Pro50Leu), p.(Ala621dup), and p.(Leu785del) FLAG-tagged CUL-4B (left panel). Levels of WDR5 in all three mutants are increased compared to WDR5 levels in WT. Levels of LIS-1 and WDR62 are normal. Tubulin is shown as control. **B**: Cycloheximide chase experiments in HEK293T cells show that novel amino acid altering variants p.(Ala621dup) and p.(Leu785del) result in an unstable protein as compared to WT,

whereas CUL-4B with the p.(Pro50Leu) change is not degraded faster. Tubulin is shown as a control. **C**: IP experiments in HEK293T cells with antibodies against CUL-4A (upper panel) and CUL-4B (lower panel) with subsequent immunoblot of the precipitates show that WDR62 binds to CUL-4B, but not CUL-4A. DDB1 is shown as a control.

Table 1

Overview of Neuroimaging Data of Patients with *CUL4B* Variants

Family	**1**	**1**	**1**	**2**	**3**	**4**	**5**	**5**	**5**	**6**	**6**	**9**	**10**	**10**	**11**
Individual	IV:3	III:3	II:3	III:1	III:1	III:1	III:5	III:1	III:2	III:1	III:2	IV:1	II:1	II:2	II:2
Variant	p.(Leu864 Alafs*13)	p.(Leu864 Alafs*13)	p.(Leu864 Alafs*13)	p.(Leu785 del)	p.(Ala621 dup)	p.(Ile336 Lysfs*2)	SS exon 20	SS exon 20	SS exon 20	p.(Gly788 Trpfs*4)	p.(Gly788 Trpfs*4)		p.(Pro50 Leu)	p.(Pro50 Leu)	p.(Gln876*)
Neuroimaging studies	MRI and CT	LPEG	LPEG	MRI	MRI	MRI	CT	MRI	MRI	CT	MRI	CT	MRI	MRI	MRI
Age at study	1 and 6 weeks	6 Weeks	14 Years	2 Years, 3 months	Adult	2 Years, 10 months	1 Year, 10 months	45 Years	40 Years	14 Years	9 Years	8 Years	2 Years, 6 months	6 Months	13 Days and 11 months
Severity of abnormalities	+++	+++	+++	+	−	++	−	+	+	−	−	−	+++	+++	++
Cortical malformations	Bilateral perisylvian PMG	N/A	N/A			Cortical dysplasia parietal right	N/A			N/A	N/A	N/A	Slightly thick and undersulcated	Very simplified gyral pattern	Bilateral perisylvian PMG
Ventriculomegaly	+++	+++	+++	+	−	−	−	−	+	−	−	−	+++	+++	+
Diminished white matter	N/A	N/A	N/A	±	−	N/A	N/A	+	±	N/A	N/A	N/A	+++	+++	++
Other	Persistent cavum septum pellucidum			Thin CC		Enlarged right fissure of Sylvius, cavum veli interpositi		Cerebellar mid-vermian atrophy					Thin, arched CC, small thalami, hippocampi, and ventral pons	Thin, arched CC, small pons, and cerebral peduncles	Geminolytic cyst, small anterior lobe of cerebellar vermis

CC, corpus callosum; CT, computed tomography; (L) PEG, (lumbar) pneumoencephalography; MRI, magnetic resonance imaging; N/A, not assessable; PMG, polymicrogyria; SS, splice site +++, severe; ++, moderate; +, mild; +/− borderline.

Table 2

Overview of Clinical Data of Presently and Previously Described Families with CUL4B Variants

	Family	1 (N151)	2 (D112)	3 (P142)	4 (N146)	5 (D173)	6 (D203)	7 (D102)	8 (D287)	9 (GOLD506)	10 (P307)	11	Total new	Previous total	Total
	No. of affecteds	3	3	2	2	3	3	2	2	2	2	1	25	60	85
	Variant	c.2590_2593 del	c.2353_2355 del	c.1860_1862 dup	c.1007_1011 del	c.2493+3 A>G	c.2361dup	c.1906+1 G>T	c.481_482 del	del 119,578,701–119,584,448	C.149C>T	C.2626C>T	11	13	24
	Protein change	p.(Leu864Ala fs*13)	p.(Leu785 del)	p.(Ala621 dup)	p.(Ile336Lys fs*2)	SS exon 20	p.(Gly788 Trpfs*4)	canonical SS exon 15	p.(Serl61Tyr fs*24)		p.(Pro50Leu)	p.(Gln876*)			
	Ages (years)	10, 28, 37	8, 22, 28		14, 36	30, 40, 45	9, 14, 38	39, 41	15, 17	11, 37	2, 4	4			
Growth	Birth weight <p10	1/2	1/3	NR	0/1	2/3	1/2	NR	1/2	1/1	1/2	0/1	8/16 (50%)	16/26 (62%)	57%
	Height <p10	3/3	1/3	NR	2/2	3/3	2/3	1/1	2/2	2/2	0/2	1/1	17/22 (77%)	24/31 (77%)	77%
	Weight >p90	2/3	2/3	1/1	0/1	2/3	1/3	0/1	2/2	1/1	0/2	0/1	11/21 (52%)	19/30 (63%)	59%
	HC >p90	2/3	1/3	0/1	0/1	0/3	0/3	0/1	0/2	1/2	2/2	1/1	7/22 (32%)	11/31 (36%)	34%
CNS	MRI performed	1/3, 2× LPEG	1/3	1/2	1/2	2/3, 1× CT	1/3, 1× CT	0/2	0/2	0/2, 1× CT	2/2	1/1	10/25 (40%)	NR	40%
	CNS abnormality	3/3 +	1/1 ±	0/1	1/1 +	1/3 +, 1/3 ±	0/2	NR	NR	0/1	2/2 +	1/1 +	10/15 (67%)	1 porencephalic cyst	67%
Neurological	ID (level)	3/3 Severe	1/3 Mild; 2/3 mild-mod	1/1 mod	1/2 mod; 1/2 unknown	2/3 mod; 1/3 severe	2/3 mod; 1/3 severe	2/2 severe	1/2 mild; 1/2 mod	2/2 mod	2/2 Severe	1/1 Severe	24/24 (100%)	38/38 (100%)	100%
	Motor delay	3/3	3/3	NR	2/2	3/3	3/3	2/2	2/2	2/2	2/2	1/1	23/23 (100%)	23/23 (100%)	100%
	Speech delay	3/3	3/3	NR	2/2	3/3	3/3	2/2	2/2	2/2	2/2	1/1	23/23 (100%)	39/39 (100%)	100%
	Behavioral problems	0/2	2/3	0/1	2/2	1/3	3/3	1/1	0/2	2/2	1/2	1/1	13/22 (59%)	23/29 (79%)	71%
	Tremor	0/1	1/3	NR	2/2	3/3	2/3	0/1	0/2	1/2	0/2	0/1	9/20 (45%)	18/26 (69%)	59%
	Seizures	1/3	0/3	NR	0/2	1/3	3/3	0/1	0/2	2/2	0/2	0/1	7/22 (32%)	17/30 (57%)	46%
	Gait abnormality	2/2	0/3	NR	2/2	1/3	3/3	0/1	0/2	2/2	0/2	0/1	10/21 (48%)	15/21 (71%)	60%
Craniofacial	High/prominent forehead	2/2	1/3	1/1	0/2	3/3	3/3	NR	2/2	1/2	2/2	1/1	16/21 (76%)	NR	76%
	Family	1 (N151)	2 (D112)	3 (P142)	4 (N146)	5 (D173)	6 (D203)	7 (D102)	8 (D287)	9 (GOLD506)	10 (P307)	11	Total new	Previous total	Total
	Malformed/abnormally positioned ears	2/2	1/1	1/1	1/2	3/3	3/3	NR	2/2	2/2	1/2	1/1	17/19 (89%)	11/12 (92%)	90%
	HSR/deep-set eyes/narrow palpebral fissures	1/2	3/3	NR	2/2	3/3	3/3	0/2	2/2	2/2	1/2	0/1	17/22 (77%)	16/20 (80%)	79%
	Low nasal bridge/rounded tip	1/2	3/3	NR	2/2	1/3	2/3	0/2	2/2	0/2	2/2	1/1	12/22 (55%)	17/20 (85%)	69%
	Prominent lower lip	2/2	3/3	1/1	2/2	1/3	3/3	2/2	0/2	2/2	2/2	0/1	18/23 (78%)	16/28 (57%)	67%
	Prognathia	2/2	3/3	NR	1/2	3/3	3/3	NR	0/2	1/1	0/2	0/1	13/19 (68%)	NR	68%
	Hypogonadism/genital abnormalities	3/3	1/1	0/1	1/1	3/3	3/3	1/1	2/2	2/2	0/2	1/1	17/20 (85%)	22/34 (65%)	72%
Extremities	Brachydactyly/small hands/small feet	0/2	2/2	NR	2/2	3/3	3/3	0/1	2/2	2/2	0/2	NR	14/19 (74%)	24/31 (77%)	76%
	Wasted lower leg muscles	2/2	NR	NR	0/1	0/3	1/2	1/1	NR	1/2	NR	NR	5/11 (45%)	7/12 (58%)	52%
	Pes cavus	NR	NR	NR	0/1	0/3	1/2	0/1	NR	1/2	0/2	0/1	2/11 (18%)	10/19 (53%)	40%
Other	Gynecomastia	0/1	NR	1/1	0/1	3/3	1/3	0/2	0/2	1/2	0/2	0/1	6/18 (33%)	7/10 (70%)	46%
	Kyphosis	0/2	NR	NR	2/2	1/3	1/3	0/2	0/2	1/2	NR	1/1	6/17 (35%)	9/27 (33%)	34%

Family	1 (N151)	2 (D112)	3 (P142)	4 (N146)	5 (D173)	6 (D203)	7 (D102)	8 (D287)	9 (GOLD506)	10 (P307)	11	Total new	Previous total	Total
Other	Diaphragmatic hernia, bilateral inguinal hernia, short humeri	Pes adductus		Strabism, torticollis, keratoconus	Strabism, pes planus	Strabism, astigmatism, macrostomia, hypoacusis		Synophrys	Prominent incisors		Brown syndrome			

CUL4B reference sequence NM_003588.3, NP_003579.3.

CNS, central nervous system; CT, computed tomography; H, hydrocephalus HC, head circumference; HSR, hyperplastic supraorbital ridges; ID, intellectual disability; MCD, malformations of cortical development; mod, moderate; mod, moderate; MRI, magnetic resonance imaging; NR, not reported; SS, splice site